Volume 15, Issue 1, 152507 (1-8)

Iranian Journal of Catalysis (IJC)

https://doi.org/10.57647/j.ijc.2025.1501.07

Fe_3O_4@nano-coconut shell/Cu(II): A unique and reusable catalyst for green synthesis of naphtho[1,3]oxazine derivatives

Farhad Hajati, Bi Bi Fatemeh Mirjalili*

Department of Organic Chemistry, Faculty of Chemistry, College of Science, Yazd University, Yazd, Iran.

***Corresponding author:** fmirjalili@yazd.ac.ir

Original Research

Received:
23 March 2024
Revised:
28 October 2024
Accepted:
12 December 2024
Published online:
8 January 2025

Abstract:

Coconut shell nanoparticles were transformed into magnetic nanoparticles (Fe_3O_4@nano-coconut shell) that were utilized for Lewis acid (Cu(II)) support. Consequently, the synthesis of the Fe_3O_4@nano-coconut shell/Cu(II) catalyst, possessing easy and complete recovery capabilities, was achieved. The characterization of Fe_3O_4@nano-coconut shell/Cu(II) was conducted using various techniques, including FT-IR, FESEM, VSM, EDS-MAP, XRD, BET, and TGA. The catalytic efficacy of Fe_3O_4@nano-coconut shell/Cu(II) as a potent Lewis acid nano-catalyst was assessed for the manufacture of 2-aryl-2, 3-dihydro-1H-naphtho[1, 2-e][1, 3]oxazine derivatives via a reaction of formaldehyde, aniline derivatives, and phenolic substrate such as β-naphthol. Fe_3O_4@nano-coconut shell/Cu(II) demonstrated robust performance in the reaction and could be reused up to four consecutive times with only a minor decline in catalytic activity.

Keywords: Fe_3O_4@nano-coconut shell/Cu (II); Green chemistry; Magnetic nanoparticles; Multi-component reactions; 1, 3-Oxazine

1. Introduction

Multicomponent reactions (MCRs) offer advantages in selectivity, simplicity, and effectiveness over traditional multi-step synthesis methods [1–3]. For this reason, MCRs have received considerable interest in organic chemistry, like combinational chemistry or pharmacochemistry [4, 5].
Nowadays, magnetic nanoparticles (MNPs) have expanded due to their special physical and chemical properties, high surface area and high penetration power [6, 7]. Recently, various coating techniques for Fe_3O_4 noparticles such as carbon, [8] surfactants, [9] biopolymers [10, 11] and silica [12, 13] have been used. The most common method for the synthesis of various naphthol [1, 2-e][1, 3]oxazines is the multi-component reaction of 2-naphthol, formaldehyde and a primary amine via a Mannich-type condensation. Recently, several catalysts such as alum ($KAl(SO_4)_2.12\ H_2O$), [14] PEG-400, [15] Thiamine hydrochloride (VB_1), [16] $ZrOCl_2.8H_2O$, [17], GA-OPO_3H_2 [18] and CCl_3COOH [19] have been used for this reaction.
Yet, several existing procedures come with drawbacks such as high costs, extended reaction times, reliance on toxic organic solvents, and low product yields [20, 21]. Thus, emphasis has been placed on adopting safe and environmentally friendly methods for the preparation of 1, 3-oxazine derivatives. Recently, there has been a growing interest in utilizing non-toxic, eco-friendly solvents like water as alternatives to volatile organic solvents [22, 23].
The nano-coconut shell, being a natural biopolymer, presents itself as an ideal coating layer for Fe_3O_4 nanoparticles. This coating not only stabilizes the nanoparticles in solution but also provides free OH groups, facilitating functionalization for various purposes. In this study, Fe_3O_4@nano-coconut shell/Cu(II) was synthesized as a natural-based nano-magnetic catalyst, and its effects were considered in the reaction of amines, formaldehyde and β-naphthol for the synthesis of 1, 3-naphthoxazine derivatives.

2. Experimental

2.1 General

Chemical materials were prepared by Neutron and Merck companies. The FTIR of products was recorded by Bruker, Equinox 55 spectrometer. The ^{1}H-NMR spectra were obtained on a Bruker (DRX-400 Avance) NMR. Melting points were measured on a Buchi melting point B-540 B.V.CHI instrument. X-ray diffraction (XRD) pattern was obtained by a Philips Xpert MPD diffract meter equipped with a Cu Kα anode (k = 1.54 Å) in the 2θ range from 10 to 80 °. Field Emission Scanning Electron Microscopy (FESEM) was recorded by a Mira 3-XMU. XRF analysis was done with Bruker, S4 Explorer instrument. The magnetization of the prepared catalyst was characterized by using a Vibrating Sample Magnetometer (Meghnatis Daghigh Kavir Co. Kashan, I.R.IRAN). Quantitative elemental information and maps of the catalyst were analyzed using energy-dispersive X-ray spectroscopy (EDX) with a Phenom Pro X instrument. The specific surface area of the catalyst was determined at 77 K using a BELSORP MINI II nitrogen adsorption apparatus from Japan, recording the Brunauer-Emmett-Teller (BET) data.

2.2 Preparation of nano-coconut shell

To prepare the nanococonut shell, it was initially heated in boiling water for 30 minutes, then dried and ground into powder. Next, the powdered shell was treated with a 17.5% w/v NaOH solution at 90 °C for 24 hours under reflux conditions. Afterwards, the coconut shell was filtered and rinsed with distilled water. Following that, it underwent bleaching with a 1:1 aqueous dilution of 3.5% w/v sodium hypochlorite (NaOCl) at 80 °C for 3 hours under reflux conditions. The resulting powder was then partially hydrolyzed using a 35% sulfuric acid (H_2SO_4) aqueous solution with a coconut shell-to-acid weight ratio of $1-10$ at 45 °C. After 3 hours, the suspension was diluted five-fold with water to halt the hydrolysis reaction. Finally, the suspension was centrifuged at 4000 rpm to separate the nano-coconut shell from the acidic medium (yield 65%).

2.3 Preparation of Fe_3O_4@nano-coconut shell

1.5 g of nano-coconut shell powder was poured into 100 mL of 0.05 M acetic acid solution. Then, $FeCl_3.6H_2O$ (3.51 g, 0.013 mol) and $FeCl_2.4H_2O$ (1.29 g, 0.0065 mol) were added to it. The mixture was stirred for 6 h at 80 °C. As a result, 6 mL of 25% NH_4OH was added dropwise into the reaction mixture with constant stirring. After 30 min, the mixture was cooled to room temperature. Then, Fe_3O_4@nano-coconut shell was collected by an external magnet, washed with distilled water and dried at 80 °C for 4 h. The weight of the nano-Fe_3O_4@almond shell obtained is 2.073 g.

2.4 Preparation of Fe_3O_4@nano-coconut shell/Cu(II)

A mixture of $CuCl_2$ (75 mL, 0.04 M), Fe_3O_4@nano-coconut (1 g) and ethanol (20 mL) was stirred at room temperature for 6 hours. The resultant magnetic nanocatalyst underwent washing with ethanol and water and then dried in an oven at 80 °C.

2.5 General procedure for synthesis of naphtho[1, 2-e][1, 3]oxazine derivatives:

A mixture of Fe_3O_4@nano-coconut shell/Cu(II) (0.05 g), primary amine (1.0 mmol), β-naphthol (1.0 mmol) and formaldehyde (2.0 mmol) was stirred for 15 min at room temperature. The completion of the reaction was checked by TLC (ethyl acetate: n-hexane (1:4)). The reaction mixture was dissolved in 5 mL of hot ethanol, and the magnetic nano-catalyst was separated using an external magnet. Cold water was then added to the reaction mixture, and the solid product was collected via filtration. The recovered catalyst underwent three washes with hot ethanol, followed by drying, and was subsequently reused for subsequent runs.

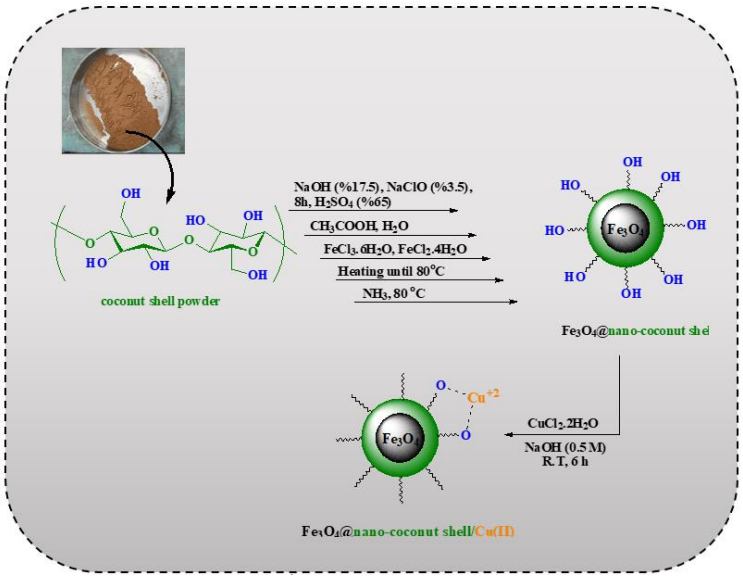

Scheme 1. Preparation of Fe_3O_4@nano-coconut shell/Cu(II).

3. Results and discussion

The preparation steps of Fe_3O_4@nano-coconut shell/Cu(II) were shown in Scheme 1.

For the identification of the structure of Fe_3O_4@nano-coconut shell/Cu(II), FT-IR (ATR) spectra of (a) coconut shell, (b) Fe_3O_4@nano-coconut shell, and (c) Fe_3O_4@nano-coconut shell/Cu(II) were recorded (figure 1). The FT-IR spectrum of the nanococonut shell shows a broad band at $3250-3450\ cm^{-1}$, which is related to the stretching vibrations of OH groups. The absorption band at $2950\ cm^{-1}$ is attributed to C-H aliphatic bonds. The absorption band around $1044\ cm^{-1}$ is due to the C–O bonds stretching vibrations. For the Fe_3O_4@nano-coconut shell, the absorption at $624\ cm^{-1}$ indicates the Fe/O groups stretching vibrations that show the magnetic Fe_3O_4 is coated by a nano-coconut shell. The peak at $1504\ cm^{-1}$ is associated with the bending vibration of H–O–H that catalyses adsorbed water [24]. The absorption bands at $691\ cm^{-1}$ may be attributed to the Cu-O band.

To clarify, the morphologies and sizes of the Fe_3O_4@nano-coconut shell/Cu(II), FESEM, TEM and histogram images were shown in figure 2. These results exhibit that the dimension of catalyst particles is $20-40$ nm.

The magnetic properties of Fe_3O_4 and Fe_3O_4@nano-coconut shell/Cu(II) were studied by using a vibrating sample magnetometer (VSM) (figure 3). A superparamagnetic behaviour was achieved from the measured samples of Fe_3O_4 and the catalyst. At room temperature, the saturation magnetization (Ms) values of Fe_3O_4 and Fe_3O_4@nano-coconut shell/Cu(II) are 50 emu g^{-1} and 32 emu g^{-1}, respectively. The resulting values show that bonding Fe_3O_4@nano-coconut shell/Cu(II) has a considerable effect on the magnetic properties of Fe_3O_4.

The thermal gravimetric analysis (TG-DTA) pattern of the Fe_3O_4@nano-coconut shell/Cu(II) catalyst is shown in figure 4. A minor weight loss (10%) in the range of $50-280°$ can be related to removing the adsorbed water in the catalyst. The other weight losses of the catalyst, making 30% in the range of $280-380$ °C and 10% in the range of $630-650$ °C, are attributed to the burning of the carbohydrate section of the catalyst. The char yield of the catalyst at 800 °C is 39%, which confirms the existence of metal in the catalyst. Thus, the catalyst is stable up to 280 °C. and can be used

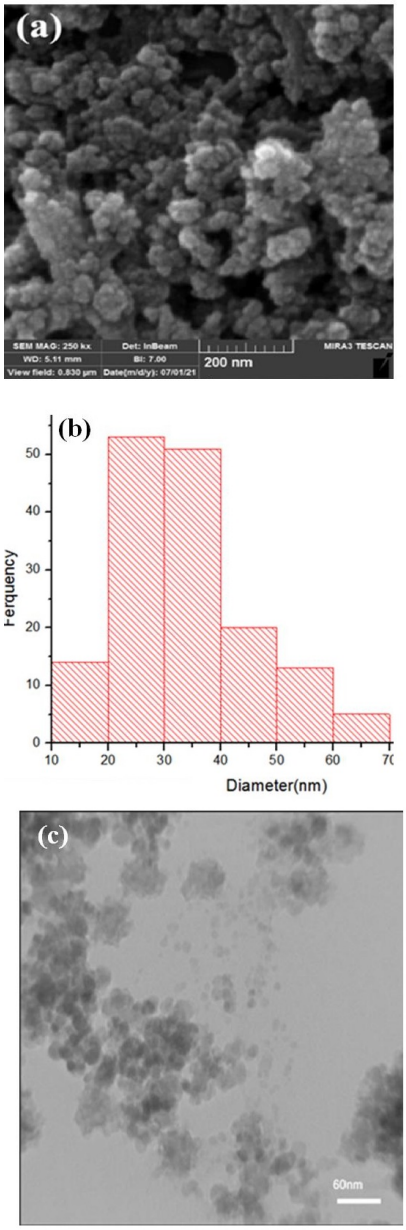

Figure 2. (a) FESEM (b) histogram and (c) TEM images of Fe_3O_4@nano-coconut shell/Cu(II).

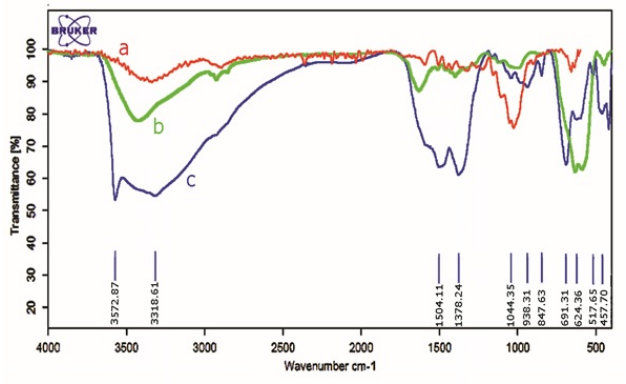

Figure 1. FT-IR spectra of (a) nano-coconut shell, (b) Fe3O4@nano-coconut shell, (c) Fe_3O_4@nano-coconut shell/Cu(II).

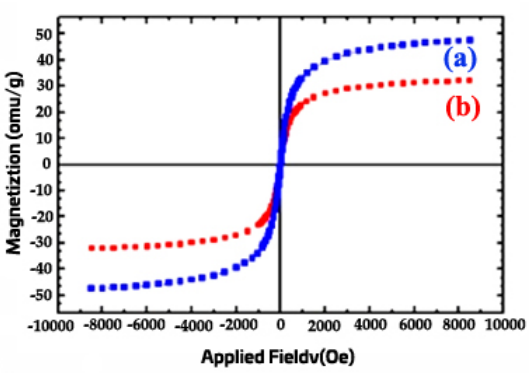

Figure 3. Magnetization loops of (a) Fe_3O_4 and (b) Fe_3O_4@nano-coconut shell/Cu(II).

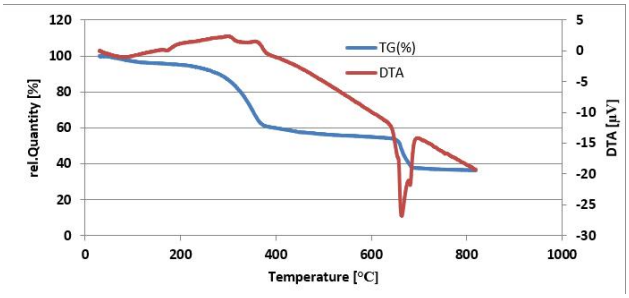

Figure 4. Thermal gravimetric analysis pattern of Fe_3O_4@nano-coconut shell/Cu(II).

under 280 °C.

By measuring the Fe and Cu content in the catalyst using Inductively Coupled Plasma (ICP), we found that the amount of Fe is 190 mg/g, and that of Cu is 100 mg/g. Thus, according to ICP, the molar ratio of Cu: Fe is 1: 1.6.

The distribution of the Fe_3O_4@nano-coconut shell/Cu(II) is also analyzed by elements mapping that shows C, O, Cl, Fe, and Cu elements are distributed homogeneously in the synthesized catalyst (figure 5).

EDX analysis was employed for the study of the chemical composition of the catalyst. This study shows the existence of C, O, Cl, Fe, and Cu in the catalyst (figure 6). In figure 6, the weight percentages of these elements are: C (20.64%), O (61.88%), Cl (1.22%), Fe (6.06%), and Cu (10.20%).

The Fe_3O_4@nano-coconut shell/Cu(II) XRD pattern in a range of $10-80$ o was shown in figure 7. In this pattern, all peaks of naked Fe_3O_4 (2θ = 30°, 37°, 43°, 53°, 57°, 63°,

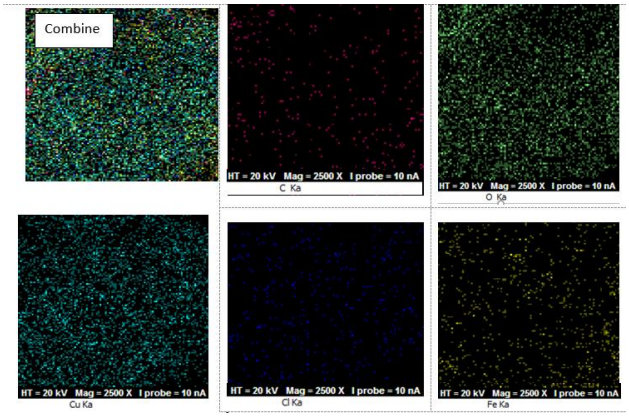

Figure 5. Elements mapping images of Fe_3O_4@nano-coconut shell/Cu(II).

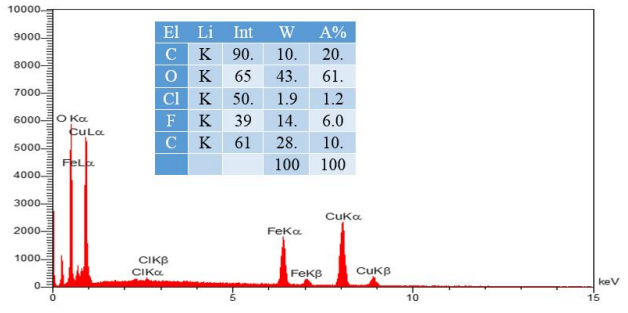

Figure 6. EDX analysis spectra of Fe_3O_4@nano-coconut shell/Cu(II).

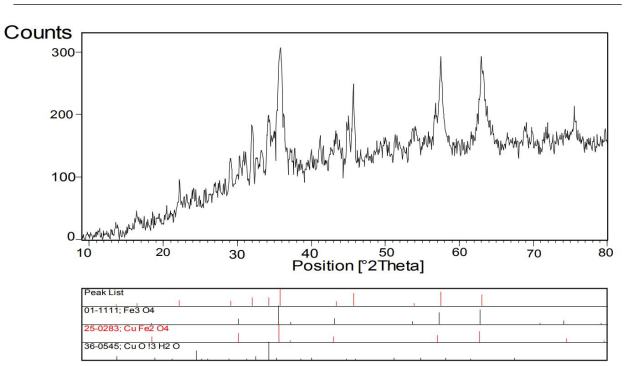

Figure 7. XRD patterns of the Fe_3O_4@nano-coconut shell/Cu(II).

71° and 73°) have been shown.

The Burunauer-Emmett-Taller specific surface area (S_{BET}) of the Fe_3O_4@nano-coconut shell/Cu(II) catalyst was measured by N_2 adsorption-desorption analysis at 77 K (figure 8 and Table 1). As shown, the N_2 adsorption-desorption isotherm for Fe_3O_4@nano-coconut shell/Cu(II) is of the II-type with H_3 hysteresis. As shown in Table 1, the surface area of particles, mean pore diameters, and total pore volume were 36.6 $m^2.g^{-1}$, 18.107 nm, and 0.1657 $cm^3.g^{-1}$, respectively.

The efficiency of Fe_3O_4@nano-coconut shell/Cu(II) was justified for the synthesis of naphtho[1, 2-e][1, 3]oxazines derivatives *via* pseudo three-component reactions of β-naphthol, primary amine and formaldehyde. The synthesis of 2-phenyl-2,3-dihydro-1*H*-naphtho[1, 2-e][1, 3] oxazine was selected as a model reaction for obtaining the best condition for this protocol (Table 2). The best condition for this reaction is using 0.05 g of catalyst under solvent-free conditions at room temperature (Table 2, Entry 12). Thus, according to the best condition for the synthesis of naphtho[1, 2-e][1, 3]oxazines by using Fe_3O_4@nano-coconut shell/Cu(II) as an efficient catalyst were explored, and the derivatives were obtained in good yields (Table 3). The

Table 1. Parameters obtained from porosity analysis.

BET Plot	
V_m	8.4111 [cm^3(STP)/g]
$a_{s,BET}$	36.609 [m^2/g]
C	43.125
Total pore volume(p/p_0 = 0.990)	0.1657 [cm^3/g]
Mean pore diameter	18.107 [nm]
Langmuir plot	
V_m	10.609 [cm^3(STP)/g]
$a_{s,Lang}$	46.174 [m^2/g]
B	0.2929
t plot	
Plot data	Adsorption branch
a_1	27.312 [m^2/g]
V_1	0 [cm^3/g]
BJH Plot	
Plot data	Adsorption branch
V_p	0.1698 [cm^3/g]
$r_{p,peak}$(Area)	4.61 [nm]
a_p	49.768 [m^2/g]

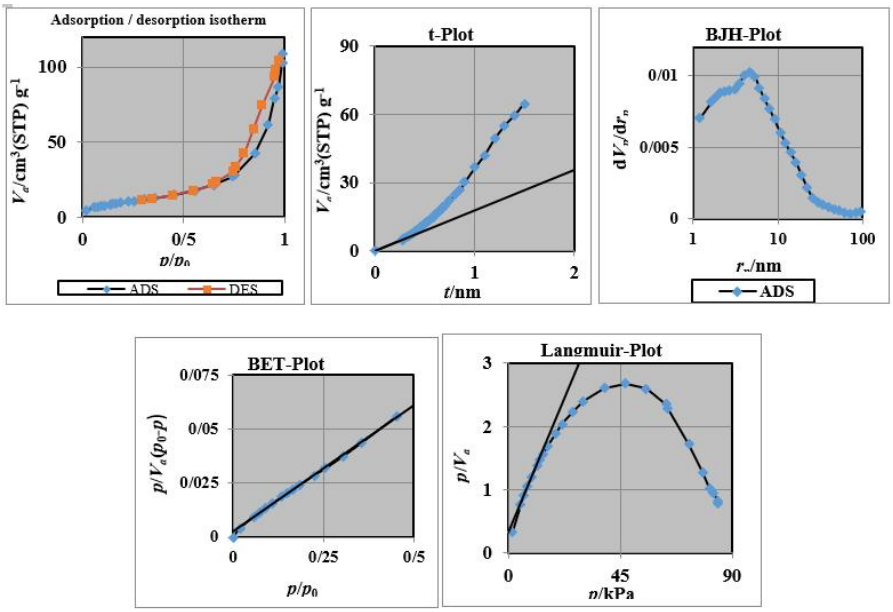

Figure 8. N_2 adsorption (black line) - desorption (orang line) isotherm and corresponding diagrams.

Table 2. Synthesis of naphtho[1, 2-e][1, 3]oxazine under various conditions[a].

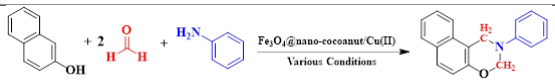

Entry	Catalyst (g)	Solvent[b](Conditions)	Time (min)	Yield[c] (%)
1	Fe_3O_4@nano-coconut shell/Cu(II) (0.05)	C_2H_5OH (r.t.)	30	68
2	Fe_3O_4@nano-coconut shell/Cu(II) (0.05)	MeOH (r.t.)	30	60
3	Fe_3O_4@nano-coconut shell/Cu(II) (0.05)	CCl_4 (r.t.)	30	63
4	Fe_3O_4@nano-coconut shell/Cu(II) (0.05)	CH_3CN (r.t.)	30	36
5	Fe_3O_4@nano-coconut shell/Cu(II) (0.05)	$CHCl_3$ (r.t.)	30	52
6	Fe_3O_4@nano-coconut shell/Cu(II) (0.05)	H_2O (r.t.)	30	62
7	Fe_3O_4@nano-coconut shell/Cu(II) (0.05)	- (60°C)	30	35
8	Fe_3O_4@nano-coconut shell/Cu(II) (0.05)	- (50°C)	30	46
9	Fe_3O_4@nano-coconut shell/Cu(II) (0.05)	- (40°C)	30	63
10	Fe_3O_4@nano-coconut shell/Cu(II) (0.08)	- (r.t.)	15	79
11	Fe_3O_4@nano-coconut shell/Cu(II) (0.06)	- (r.t.)	15	97
12	Fe_3O_4@nano-coconut shell/Cu(II) (0.05)	- (r.t.)	15	97
13	Fe_3O_4@nano-coconut shell/Cu(II) (0.04)	- (r.t.)	20	95
14	Fe_3O_4@nano-coconut shell/Cu(II) (0.03)	- (r.t.)	20	80
15	Fe_3O_4@nano-coconut shell/Cu(II) (0.00)	- (r.t.)	120	None

[a]The molar ratios are β-naphthol (1 mmol), anilin (1 mmol) and formaldehyde (2 mmol)
[b]Solvents (1 ml)
[c]Isolated yield.

presence of a strong electron-withdrawing group, such as NO_2, on the para-position of aniline reduces its reactivity as a nucleophile, resulting in a decreased yield of product (Table 3, Entry 14).

In this protocol, the factor of reusability for the catalyst was taken into account. After each run, the catalyst was separated by an external magnet and washed with chloroform. The results indicated that the catalyst could be reused for up to five times without any significant loss of its activity (Fig. 9).

The structure of the reused catalyst was studied by FTIR. The comparison between fresh and reused catalysts shows no difference between them (Fig. 10).

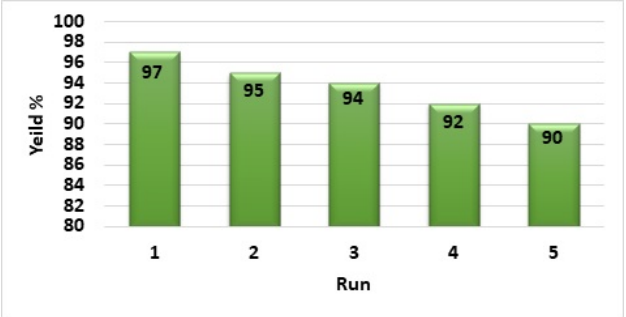

Figure 9. Recycling experiment.

Table 3. Fe_3O_4@nano-coconut shell/Cu(II) catalyzed synthesis of naphtho[1, 2-e][1, 3]oxazine.

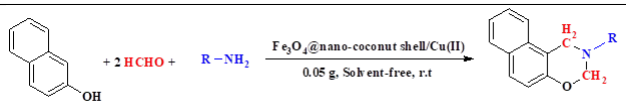

Ent.	R	Prod.	Time (min)	Yield (%)[b]	M.P.(°C)	Lit. M.P (°C) [Refs.]
1	Ph-	4a	15	97	47 – 49	46 – 58 [14]
2	4-Me-Ph-	4b	12	92	87 – 89	87 – 89 [14]
3	4-Et-Ph-	4c	12	90	43 – 46	43 – 46 [25]
4	4-Br-Ph-	4d	10	93	116 – 118	118 – 120 [26]
5	4-Cl-Ph-	4e	10	91	100 – 104	100 – 104 [16]
6	4-OMe-Ph-	4f	7	92	76 – 78	76 – 78 [16]
7	Ph-CH_2-	4g	8	90	125 – 127	123 – 125 [26]
8	2-Cl-Ph-CH_2-	4h	10	88	70 – 75	70 – 75 [25]
9	Ph-CH_2-CH_2-	4i	7	93	232(d)	232(d) [25]
10	2-Furyl-CH_2-	4j	8	92	98 – 100	98 – 100 [25]
11	Cyclohexyl-	4k	8	94	248(d)	248(d) [25]
12	n-butyl-	4l	7	93	170(d)	170(d) [25]
13	n-hexyl-	4m	7	91	177(d)	177(d) [27]
14	4-NO_2-Ph-	4n	40	$\leq$10	-	165 – 167 [28]

[a]Reactions Conditions: primary amine (1) (1 mmol), formaldehyde (2) (2 mmol), β-naphthol (3) (1 mmol)
[b]Isolated yield of pure products.
d: decompose

The suggested mechanism for synthesis of naphtho[1, 2-e][1, 3]oxazine catalyzed by Fe_3O_4@nano-coconut shell/Cu(II) was indicated in Scheme 2. Cu(II) in Fe_3O_4@nano-coconut shell/Cu(II) operates as a Lewis acid and first activates the carbonyl functional group in formaldehyde and the formed imine (3). After condensation between 2-naphthol and imine (3), the intermediate (4) was formed, which converted to the enol form of (5). In the final, the oxazine product was formed by cyclization of (5). In the next step, to show the competency of the present work versus the previously reported results in the literature, the model reaction has been compared in Table 4. As Table 4 determines, the yield or the time of the reaction in our work is shorter than that in other previously reported methods. This can perhaps be credited to the higher local concentration

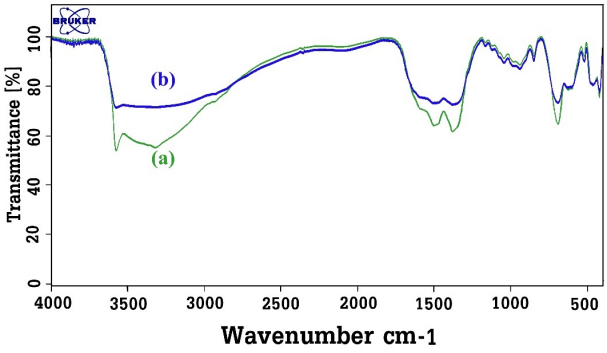

Figure 10. FT-IR spectra of (a) fresh Fe_3O_4@nano-coconut shell/Cu(II), (b) reused Fe_3O_4@ nano-coconut shell/Cu(II).

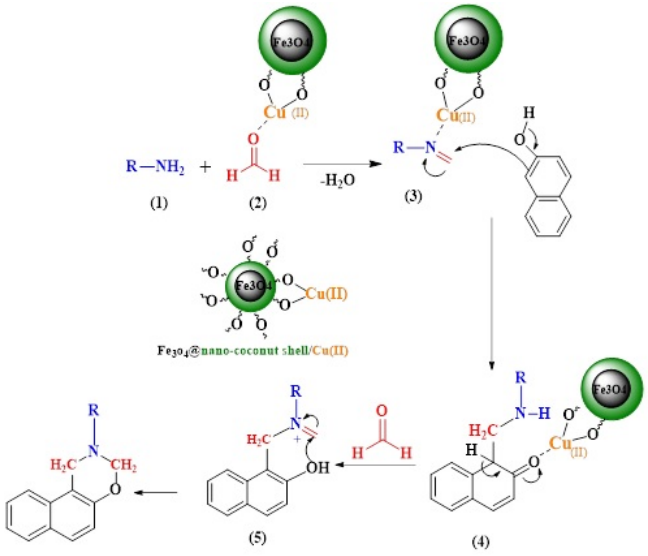

Scheme 2. Proposed mechanism for the formation of naphtho[1, 2-e][1, 3]oxazine derivatives catalyzed by Fe_3O_4@nano-coconut shell/Cu(II).

Table 4. Comparison Fe_3O_4@nano-coconut shell/Cu(II) with to other catalysts in the model reaction.

Entry	Catalyst	Solvent	Condition	Time (min)	Yeld (%)[a]	Ref.
1	Nano-$Al_2O_3/BF_3/Fe_3O_4$	H_2O	r.t	20	90	[25]
2	Nano-Fe_3O_4@walnut shell/Cu(II)	-	60 °C	25	93	[27]
3	-	Glycerol	40 °C	8 – 10	76	[29]
4	Thiamine hydrochloride	H_2O	r.t	30	92	[30]
5	GO-Fe_3O_4-Ti(IV)	-	60 °C	20	91	[31]
6	FNAOSiPAMP/Cu(II)	-	r.t	25	99	[32]
7	Iron(III) trifluroacetate	H_2O.SDS	r.t	25	86	[33]
8	Fe_3O_4@nano-cocoanut shell/Cu(II)	-	r.t	15	97	A[b]

[a]Isolated yield
[b]A: This work (Table 3, entry 1)

of catalyst species inside the pores insomuch, in fact, the reaction occurs on the surface or in the pores of the catalyst. Accordingly, we believe that in comparison with some other recent reports accessible in the literature, the present method is an improvement with respect to other procedures.

Conclusion

In conclusion, in this article, we have reported a facile method for the synthesis of naphtho[1, 2-e][1, 3]oxazine derivatives using Fe_3O_4@nano-coconut shell/Cu(II) as a new magnetic natural-based nano-catalyst. This procedure was done at room temperature under solvent free condition. The newly synthesized catalyst has shown good utility following the product yields, simple separation, and benign reaction conditions.

Acknowledgements
The authors thank the Research Council of Yazd University for the support of this research.

Supporting Information
The FTIR and NMR of products were recorded as supporting information.

Authors contributions
Authors were contributed equally to prepare the paper.

Availability of data and materials
The data supporting this study are available from the corresponding author on request.

Conflict of interests
The authors declare that they have no interest in influencing the work reported in this paper.

References

[1] T. Ahmadi, G. M. Ziarani, P. Gholamzadeh, and H. Mollabagher. *Tetrahedron: Asym*, **28**(2017):708–724.
DOI: https://doi.org/10.1016/j.tetasy.2017.04.002.

[2] C. Hulme, S. Chappeta, C. Griffith, Y. S. Lee, and J. Dietrich. *Tetrahedron Lett.*, **50**(2009):1939–1942.
DOI: https://doi.org/10.1016/j.tetlet.2009.02.099.

[3] S. Verma, S. L. Jain, and B. Sain. *Tetrahedron Lett.*, **51**(2010):6897–6900.
DOI: https://doi.org/10.1016/j.tetlet.2010.10.124.

[4] K. Tanaka and F. Toda. *Chem. Rev.*, **100**(2000):1025–1074.
DOI: https://doi.org/10.1021/cr940089p.

[5] Z. L. Shen and S. J. Ji. *Synth. Commun.*, **39**(2009):775–791.
DOI: https://doi.org/10.1080/00397910802431149.

[6] L. H. Reddy, J. L. Arias, J. Nicolas, and P. Couvreur. *Chem. Rev.*, **112**(2012):5818–5878, .
DOI: https://doi.org/10.1021/cr300068p.

[7] K. Zhou, X. Zhou, J. Liu, and Z. Huang. *J. Pet. Sci. Eng*, **188**(2020): 106943.
DOI: https://doi.org/10.1016/j.petrol.2020.106943.

[8] S. Zhang, H. Niu, Z. Hu, Y. Cai, and Y. Shi. *J. Chromatogr. A*, **1217**(2010):4757–4764, .
DOI: https://doi.org/10.1016/j.chroma.2010.05.035.

[9] K. Khoshnevisan, M. Barkhi, D. Zare, D. Davoodi, and M. Tabatabaei. *Synth. React. Inorg. Met-Org. Chem.*, **42**(2012): 644–648.
DOI: https://doi.org/10.1080/15533174.2011.614997.

[10] J. Safari and L. Javadian. *RSC Adv.*, **4**(2014):48973–48979.
DOI: https://doi.org/10.1039/C4RA06618A.

[11] V. A. J. Silva, P. L. Andrade, M. P. C. Silva, L. D. L. S. Valladares, and J. A. Aguiar. *J. Magn. Magn. Mater.*, **343**(2013):138–143.
DOI: https://doi.org/10.1016/j.jmmm.2013.04.062.

[12] V. Polshettiwar, R. Luque, A. Fihri, H. Zhu, M. Bouhrara, and J. M. Basset. *Chem. Rev.*, **111**(2011):3036–3075.
DOI: https://doi.org/10.1021/cr100230z.

[13] R. B. Nasir Baig and R. S. Varma. *Ind. Eng. Chem. Res.*, **53**(2014): 18625–18629.
DOI: https://doi.org/10.1021/ie501081q.

[14] S. A. Sadaphal, S. S. Sonar, B. B. Shingate, and M. S. Shingare. *Green. Chem. Lett. Rev.*, **3**(2010):213–216.
DOI: https://doi.org/10.1080/17518251003709522.

[15] P. V. Shinde, A. H. Kategaonkar, B. B. Shingate, and M. S. Shingare. *Chin. Chem. Lett.*, **22**(2011):915–918.
DOI: https://doi.org/10.1016/J.CCLET.2011.01.011.

[16] V. D. Dhakane, S. S. Gholap, U. P. Deshmukh, H. V. Chavan, and B. P. Bandgar. *C. R. Chim.*, **17**(2014):431–436, .
DOI: https://doi.org/10.1016/j.crci.2013.06.002.

[17] M. S. Al-Ajely and A. M. Noori. *Bio med. J. Sci. Tech. Res.*, **29**(2020): 22510–22516.
DOI: https://doi.org/10.26717/BJSTR.2020.29.004815.

[18] S. S. Hosseinikhah, B. B. F. Mirjalili, N. Salehi, and A. H. Bamoniri. *RSC. Adv.*, **10**(2020):40508–40513.
DOI: https://doi.org/10.1039/D0RA07199D.

[19] R. Borah, A. K. Dutta, P. Sarma, C. Dutta, and B. Sarma. *RSC Adv.*, **4**(2014):10912–10917.
DOI: https://doi.org/10.1039/C3RA47211F.

[20] C. S. Higham, D. P. Dowling, J. L. Shaw, A. Cetin, C. J. Ziegler, and J. R. Farrell. *Tetrahedron lett.*, **47**(2006):4419–4423.
DOI: https://doi.org/10.1016/j.tetlet.2006.04.077.

[21] W. J. Burke, E. M. Glennie, and C. Weatherbee. *Org. Chem.*, **29**(1964):909–912.
DOI: https://doi.org/10.1021/jo01027a038.

[22] R. A. Sheldon. *Green. Chem.*, **7**(2005):267–278.
DOI: https://doi.org/10.1039/B418069K.

[23] M. Zhang, Q. Y. Fu, G. Gao, H. Y. He, Y. Zhang, Y. S. Wu, and Z. H. Zhang. *ACS Sustain. Chem. Eng.*, **7**(2017):6175–6182, .
DOI: https://doi.org/10.1021/acssuschemeng.7b01102.

[24] O. L. Keller. *Jr, Inorg. Chem.*, **2**(1963):783–787.
DOI: https://doi.org/10.1021/ic50008a029.

[25] E. Babaei and B. F. Mirjalili. *Polycycl. Aromat. Comp.*, **41**(2021): 518–525.
DOI: https://doi.org/10.1080/10406638.2019.1600561.

[26] S. S. Ganesan, N. Rajendran, S. I. Sundarakumar, Ganesan A., and B. Pemiah. *Synthesis*, **45**(2013):1564–1568, .
DOI: https://doi.org/10.1055/s-0033-1338430.

[27] A. D. Tafti and B. F. Mirjalili. *RSC Adv.*, **10**(2020):31874–31880.
DOI: https://doi.org/10.1039/D0RA04282J.

[28] M. V. Reddy, K. T. Lim, J. T. Kim, and Y. T. Jeong. *J. Chem. Res.*, **7**(2012):398–401, .
DOI: https://doi.org/10.3184/174751912X1337166261377.

[29] S. S. Ganesan, N. Rajendran, S. I. Sundarakumar, A. Ganesan, and B. Pemiah. *Synthesis*, **45**(2013):1564–1568, .
DOI: https://doi.org/10.1055/s-0033-1338430.

[30] V. D. Dhakane, S. S. Gholap, J. P. Deshmukh, H. V. Chavan, and B. P. C. R. Bandgar. *Chim.*, **17**(2014):431–436, .
DOI: https://doi.org/10.1016/j.crci.2013.06.002.

[31] S. Khabnadideh, A. solhjoo, R. Heidari, L. Amiri Zirtol, A. Sakhteman, Z. Rezaei, E. Babaei, S. Rahimi, and L. Emami. *BMC Chemistry*, **16**(2022):1–18.
DOI: https://doi.org/10.1186/s13065-022-00836-8.

[32] M. Keihanfar and B. F. Mirjalili. *Sci. Rep.*, **12**(2022):17713–17724.
DOI: https://doi.org/10.1038/s41598-022-22712-0.

[33] T. Lohar, A. Mane, S. Kamat, and R. Salunkhe. *Polycycl. Aromat. Comp.*, **40**(2020):1210–1222.
DOI: https://doi.org/10.1080/10406638.2018.1538057.